Carbohydrate Polymers 202 (2018) 488–496

Contents lists available at ScienceDirect

Carbohydrate Polymers

journal homepage: www.elsevier.com/locate/carbpol

# The three dimensional cues-integrated-biomaterial potentiates differentiation of human mesenchymal stem cells

Min Hee Park[a,c,1,2], Ramesh Subbiah[a,b,1,3], Min Jung Kwon[a], Woo Jun Kim[a,b], Sang Heon Kim[a,b], Kwideok Park[a,b,**], Kangwon Lee[c,d,*]

[a] Center for Biomaterials, Korea Institute of Science and Technology (KIST), Seoul, 02792, Republic of Korea
[b] Division of Bio-Medical Science and Technology, KIST School, Korea University of Science and Technology (UST), Seoul, 02792, Republic of Korea
[c] Department of Transdisciplinary Studies, Graduate School of Convergence Science and Technology, Seoul National University, Seoul, 08826, Republic of Korea
[d] Advanced Institutes of Convergence Technology, Gyeonggi-do, 16229, Republic of Korea

ARTICLE INFO

*Keywords:*
Bone marrow derived mesenchymal stem cells
Cell-derived matrix
Alginate
Chondrogenesis
Osteogenesis
Fibroblast-derived ECM

ABSTRACT

Alginate (Alg) hydrogels, the most popular natural biomaterials, mimic the extracellular matrix (ECM) microenvironment and offer potential biomedical applications. Despite their excellent properties such as biocompatibility, hydrophilicity and ionic crosslinking, the absence of an intrinsic cell adhesion domain lessens their cell-carrier applications in tissue engineering. Herein, we suggest a three-dimensional (3D) cell culture system by integrating Alg hydrogel and fibroblast-derived matrix (FDM). FDM including cell-adhesion motifs, signaling, and physico-mechanical cues is prepared by the decellularization process by avoiding unfavorable chemical reactions. This cues-integrated-biomaterials (CiB) 3D platform shows increased cell viability, proliferation, chondrogenic and osteogenic differentiation of human bone-marrow-derived mesenchymal stem cells (hMSCs) *in situ*. The results show that the Alg/FDM hydrogel (CiB) matrix provides an excellent microenvironment for cell adhesion and can control the differentiation of hMSCs into specific lineages. Thus, these results suggest the potential applications of the Alg/FDM hydrogel matrix as a viable 3D culture system for tissue regeneration.

## 1. Introduction

Stem cells, biomolecules such as extracellular matrix (ECM) proteins, growth factors (GFs) and biomaterials are the major and vital components in the field of tissue engineering (Lee, Silva, & Mooney, 2011; Pittenger, Mbalaviele, Black, Mosca, & Marshak, 2001; Slaughter, Khurshid, Fisher, Khademhosseini, & Peppas, 2009). Stem cells reside in the niche of various healthy tissues and have the potential of self-renewal and differentiation after trauma, disease, or aging (Blanpain, Lowry, Geoghegan, Polak, & Fuchs, 2004; Simons & Clevers, 2011). For instance, adult bone marrow contains mesenchymal stem cells (MSCs), which contribute to the regeneration of various mesenchymal tissues such as bone, cartilage, muscle, ligament, tendon, adipose, and stroma (Pittenger et al., 2001). Microenvironment cues such as various soluble factors (ECM proteins and GFs) and biophysical factors (stiffness and topography) have been found to play a critical role in directing stem cell behavior and fate (Lee et al., 2011; Subbiah et al., 2016; Trappmann et al., 2012; Wen et al., 2014). Particularly, many studies show that ECM proteins, GFs, topography, stiffness, cell size, shape, and cell-cell contact greatly affect cell behavior, function, and differentiation (Kshitiz et al., 2012; McNamara et al., 2010; Ottone et al., 2014; Reilly & Engler, 2010). Hence, it is important to understand the role of multifactorial cues and cell interaction to develop the cues-integrated-biomaterials (CiB) for successful tissue regeneration (Elbert, 2011;

* Corresponding author at: Department of Transdisciplinary Studies, Graduate School of Convergence Science and Technology, Seoul National University, Seoul, 08826, Republic of Korea.
** Corresponding author at: Center for Biomaterials, Korea Institute of Science and Technology (KIST), Seoul, 02792, Republic of Korea.
*E-mail addresses:* kpark@kist.re.kr (K. Park), kangwonlee@snu.ac.kr (K. Lee).
[1] M. H. Park and R. Subbiah contributed equally to this work.
[2] Present address: Convergence Bioceramic Materials Center, Korea Institute of Ceramic Engineering & Technology, 202 Osongsaengmyeong 1-ro, Osong-eup, Heungdeok-gu, Cheongju-si, Chungcheongbuk-do 28160, Republic of Korea.
[3] Present address: George W. Woodruff School of Mechanical Engineering; Parker H. Petit Institute for Bioengineering and Bioscience, Georgia Institute of Technology, 315 Ferst Drive NW, Atlanta, GA 30332, USA.

https://doi.org/10.1016/j.carbpol.2018.09.010
Received 30 May 2018; Received in revised form 29 August 2018; Accepted 5 September 2018
Available online 06 September 2018
0144-8617/ 

Place, Evans, & Stevens, 2009). ECM derived from cells and tissues is enriched with natural microenvironments including biomolecules, fibrous meshwork topography, and is regarded as natural CiB that offers benefits over synthetic biomaterials (Fitzpatrick & McDevitt, 2015; Subbiah et al., 2016).

The inherent three-dimensional (3D) structure of ECM acts as a stem cell niche, and are found to play a significant role on the stem cells maintenance and differentiation (Bae, Bhang, Kim, & Park, 2012; Choi et al., 2014; Gattazzo, Urciuolo, & Bonaldo, 2014; Subbiah et al., 2016). The 3D cell culture system, unlike the traditional two-dimensional (2D) system, helps to understand the dynamic interaction and functions of cells with cellular microenvironment mimicking *in vivo*-like physiological properties (Fischer, Myers, Gardel, & Waterman, 2012; Tibbitt & Anseth, 2009). Stem cell morphology, function, and differentiation show acute disparities when cultured in a 2D and a 3D matrix and suggest that emulating hierarchical biology in the conventional 2D system is insufficient due to the lack of structural architecture and the limited selection of materials (Park et al., 2014). Several 3D cell delivery carriers have been studied to induce stem cell survival and differentiation using hydrogels, porous scaffolds, and nano-fibers (Delcroix, Schiller, Benoit, & Montero-Menei, 2010; Simó, Fernández-Fernández, Vila-Crespo, Ruipérez, & Rodríguez-Nogales, 2017; Subbiah et al., 2015). Among them, hydrogel provides an excellent platform as a 3D culture matrix because the suspended cells in a polymer aqueous solution can produce cell encapsulation inside a gel by the sol-to-gel transition of the system (Simó et al., 2017). Moreover, the properties of a gel such as a modulus can be controlled by polymer concentration, compositions and cross-linking methods (Pilipchuk et al., 2013; Rehmann, Luna, Maverakis, & Kloxin, 2016; Subbiah et al., 2014). GFs can be loaded in the hydrogel easily and this system can be applied as injectable or implantable for tissue engineering (Busilacchi, Gigante, Mattioli-Belmonte, Manzotti, & Muzzarelli, 2013; Subbiah et al., 2015; Wylie et al., 2011).

Among the natural polysaccharides, alginate (Alg) is widely used as a biomaterial for tissue engineering such as cartilage and bone (Morais et al., 2013; Park & Lee, 2011; Rowley, Madlambayan, & Mooney, 1999). Alg is a naturally occurring anionic and hydrophilic polysaccharide that contains blocks of (1–4)-linked β-D-mannuronic acid (M) and α-L-guluronic acid (G) monomers (Simó et al., 2017; Yang, Xie, & He, 2011). Alg hydrogel is biocompatible, non-toxic, non-immunogenic and biodegradable, and offers various applications due to easy entrapment of cells or drugs in alg gel. However, the drawback is the lack of cell adhesion signaling moieties in Alg, which is vital for survival, proliferation, and differentiation of cells. Several studies reported the functionalization of biochemical cues such as Arg-Gly-Asp (RGD)-modified Alg hydrogels, which have been the most frequently used *in vitro* cell culture platform to date. The presence of RGD peptides in Alg hydrogels allow one to control the phenotype of interacting chondrocytes, osteoblasts, and MSCs (Degala, Zipfel, & Bonassar, 2011; Evangelista et al., 2007). However, there is still a need for the development of CiB that mimics the skeletal tissue microenvironments.

The increasing research on decellularization of tissues and cells has shown prominent success in a variety of tissue engineering applications (White et al., 2017; Willett et al., 2014). Decellularized tissues are composed of natural ECM proteins and have the advantages of maintaining the structure and topography with reduced immunogenicity, making them more attractive for allogeneic use (Crapo, Gilbert, & Badylak, 2011; Lehr et al., 2011). In addition, decellularized matrices have the potential for repair, growth, and remodeling *in vivo* (Du, Hwang et al., 2014). Our previous reports show the potential of fibroblast-derived ECM (FDM) in promoting osteogenesis, chondrogenesis, and angiogenesis (Choi et al., 2014; Du, Subbiah et al., 2014; Subbiah et al., 2016). FDM is extremely enriched with various ECM proteins such as fibronectin (FN) and type I collagen (Col I), and provides an excellent microenvironment for stem cell survival, proliferation, and differentiation. However, the mechanical property of FDM is weak, causing a lack of structural support that minimizes the widespread applications of FDM in tissue engineering. Hence, we propose the development of novel 3D CiB using Alg hydrogel and FDM, with the increased mechanical property, structural integrity, and favorable platform in this study. To investigate the biocompatibility and capacity for tissue-specific differentiation, we observed cell viability, proliferation, histology and mRNA expression. The results demonstrated that this CiB is capable of providing favorable microenvironment cues for specific differentiation of *in-situ* cultured hMSCs and envisions its use in future tissue engineering applications.

## 2. Materials and methods

### 2.1. Cell culture and preparation of FDM

hMSCs and mouse fibroblasts (NIH3T3) were obtained from Yonsei Cell Therapy Center (Seoul, Korea) and American Type Culture Collection (Manassas, VA, USA), respectively. hMSCs (passage 6) and NIH3T3 were cultured under 5% $CO_2$ atmosphere at 37 °C by using Dulbecco's modified Eagle's medium (DMEM) supplemented with 10% fetal bovine serum (FBS) containing supplement and 1% penicillin/streptomycin. The medium was replaced every third day. For FDM preparation, NIH3T3 were seeded ($2 \times 10^4/cm^2$) on cell culture dish (SPL lifescience, Korea), and cultured for 5 days until confluence. The media was changed every second day. Upon confluency, the cells were treated briefly with a detergent solution containing 0.25% Triton X-100 and 10 mM $NH_4OH$ (Sigma, USA). After the samples were washed with phosphate buffered saline (PBS), PBS containing 50 IU/mL of DNase I and 2.5 μl/mL of RNase A (Invitrogen, USA) were added to the samples and incubated at 37 °C for 2 h. Finally, the decellularized samples were gently washed twice with PBS. To prepare FDMs in suspension state, we collected decellularized FDMs from the plate (100 mm x 15 mm petri dish), added 1 mL of DMEM, then pipetted them vigorously for 5 min under cold condition using ice bath.

### 2.2. Alg/FDM preparation

Alg was prepared as a binary composition of high molecular weight (HMW) and low molecular weight (LMW) Alg. HMW Alg (PRONOVA UP MVG; Viscosity > 200 mPa*s; approximate MW ~270 kDa; with the G/M Ratio of ≤1.5) was purchased from FMC biopolymer (Norway). LMW Alg was prepared using γ-irradiation at a dose of 5 Mrad following previous study (Kong, Lee, & Mooney, 2002; Kong, Smith, & Mooney, 2003). The gel permeation chromatography (Breeze System, Waters, USA) with the multiple gel columns (Waters Ultrahydrogel Linear, Waters Ultrahydrogel 500, Waters Ultrahydrogel 250, and Waters Ultrahydrogel 120) was used to determine the average MW and polydispersity index (PDI) of both HMW and LMW Alg. 0.02 N $NaNO_3$ buffer solution was used as an eluting solvent at a flow rate of 0.8 mL/min. 1 wt.% of both HMW and LMW were mixed with chondrogenic and osteogenic induction media to prepare binary Alg precursor solution. The 1 wt.% binary Alg precursor solution was mixed with 0.15 wt.% FDM at the ratio of 4:1. The Alg/FDM solution was rapidly mixed with different concentration (100 mM, 50 mM, 25 mM and 12.5 mM) of $CaSO_4$ (Sigma, USA) slurry at 20:1 ratio for 2 min.. Enough care was taken to minimize the bubbles formation while mixing. Dual syringes and a disposable three-way stopcock (HS-T-01, Hyupsung Medical Co., Ltd, Korea) were used to thoroughly mix the solutions, as previously reported (Subbiah et al., 2015). The mixed solution was placed in the center of glass plates (20 cm X 20 cm) that was separated by 2 mm thickness spacers for 30 min. After the gelation, the disc was made using 8 mm ø biopsy puncher. The volume of each disc was measured to be 100 μL, which was then incubated at standard culture condition.

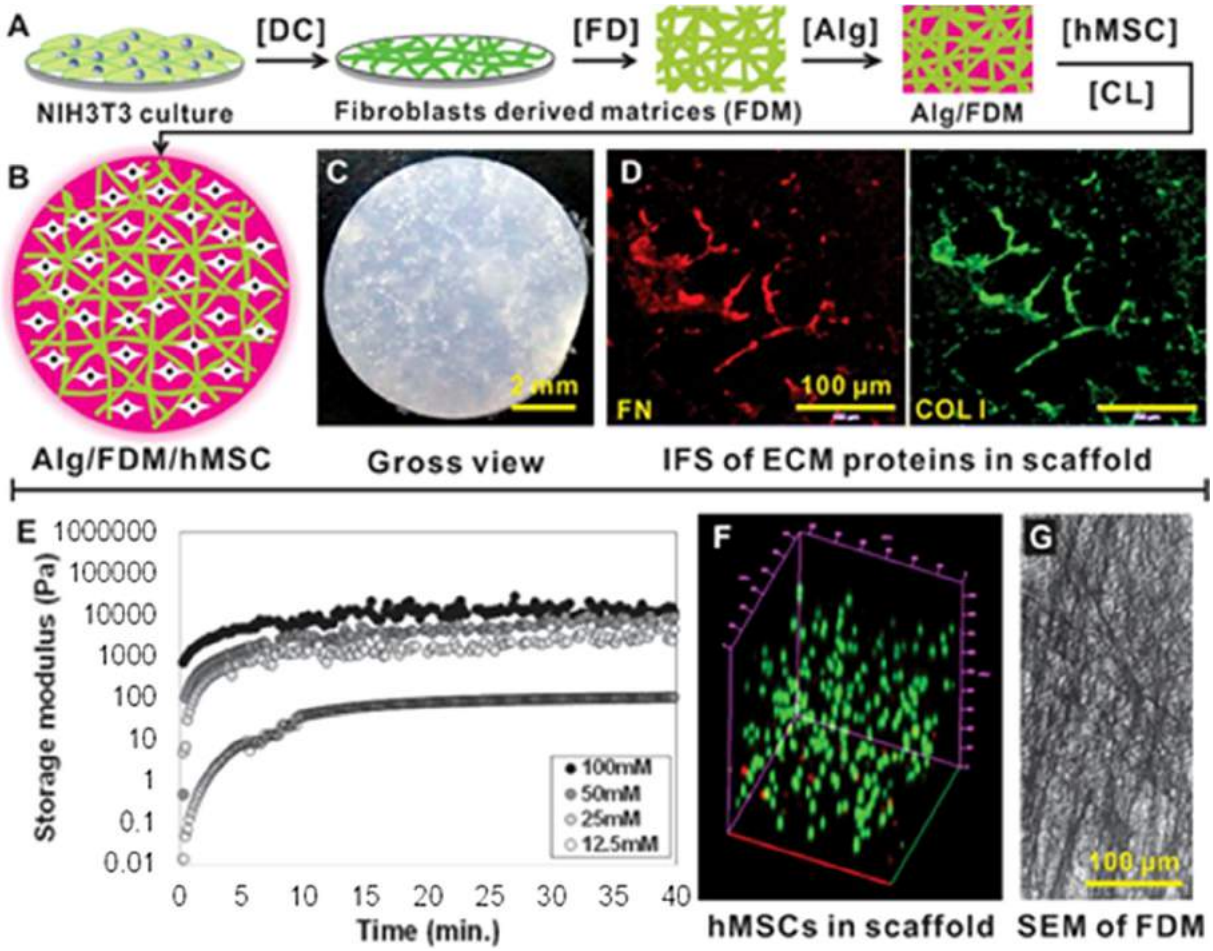


**Fig. 1.** The schematic depicts preparation of FDM (A), alginate/FDM (Alg/FDM) CiB and fabrication of hybrid disc (B) which consists of Alg/FDM and hMSCs, wherein DC, FD, CL indicate decellularization, freeze drying, and cross-linking, respectively (scale bar = 500 μm). (C) Gross view of freshly prepared Alg/FDM with hMSCs. (D) The biomarkers for extracellular matrix protein such as fibronectin (FN) and collagen type I (COL I) are shown. (E) Storage modulus of the alginate hydrogel (Alg) as a function of the $CaSO_4$ cross-linking at 37 °C. (F) Distribution of hMSCs within Alg hybrid disc analyzed by the live/dead cell assay. (G) SEM image indicates the highly organized micro-nano network of FDM.

### 2.3. Dynamic mechanical analysis

The storage modulus of the Alg and Alg/FDM disc was investigated by dynamic rheometry (Rheometer RS 1; Thermo Haake) at room temperature. The hydrogel disc was placed between parallel plates with 25 mm in diameter and a gap of 0.5 mm. During the dynamic mechanical analysis, the samples were placed inside a chamber with water-soaked cotton to minimize water evaporation. The data were collected under controlled stress (4.0 dyn/cm$^2$) and frequency of 1.0 rad/s.

### 2.4. D cell culture

hMSCs were cultured in DMEM containing 10% fetal bovine serum and 1% penicillin/streptomycin under a 5% $CO_2$ atmosphere at 37 °C and were subcultured to passage 5. As schematically illustrated in Fig. 1A and B, the harvested cells (passage 6, $1 \times 10^6$ cells/mL) were mixed respectively with Alg and Alg/FDM aqueous solution prior to crosslinking. These prepared solutions were then mixed with cross-linking agent (50 mM $CaSO_4$ slurry) thoroughly in the same manner. Enough care was taken during each mixing step to avoid the formation of bubbles. The discs were then made using casting method and biopsy punch as discussed earlier and incubated in 24 well culture plates at 37 °C using respective culture condition. The final cell seeding density was estimated to be $1 \times 10^5$ cells per disc. For chondrogenic differentiation studies, hMSCs were cultured in hydrogel using DMEM/F12 supplemented with 50 mg/mL ascorbate, 0.1 mM dexamethasone, 40 mg/mL L-proline, 100 mg/mL sodium pyruvate, ITS-plus (Collaborative Biomedical Products, Cambridge, MA, USA), antibiotics, and 10 ng/mL recombinant human transforming growth factor-β1 (TGF-β1, R&D Systems, USA). Osteogenic induction was accomplished using α-MEM supplemented with 10% FBS, 50 mg/mL ascorbate, 10 mM β-glycerophosphate, 0.1 mM dexamethasone, and antibiotics. All cultures were maintained for 28 days in a humidified incubator at 37 °C and 5% $CO_2$ with media changes every 3 days.

### 2.5. Cell proliferation and viability

The proliferation of hMSCs in hydrogels was determined using Cell Counting Kit (CCK)-8 method as previously described (Subbiah et al., 2016). The CCK-8 solution (Dojindo, Japan) was added to each well, after 2 h of incubation, the absorbance was measured at 450 nm using Multiskan Spectrum (Thermo Fisher Scientific, USA). For the live-dead cell assay, hMSCs in hydrogels were stained using the Live-Dead Cell Staining Kit (BioVision, Korea) for 30 min according to the manufacturer's protocol. The fluorescently labeled cells were finally observed under an LSM 700 laser scanning confocal microscope (Zeiss, Germany).

### 2.6. Histology and immunofluorescence staining

For chondrogenic and osteogenic differentiation, the Alg and Alg/FDM with hMSCs were fixed in 4% ρ-formaldehyde for histological evaluation. Then, they were embedded in the optimal cutting temperature (OCT) compound (Sakura® Fineteck, USA), followed by sectioning. The sections were stained with alcian blue, alizarin red, and von Kossa staining. Blue, red and black or brownish-black colored spots were visualized *via* optical microscopy (Carl Zeiss Axio Vert. A1 Microscope, Germany). For the immunofluorescence study to measure expression levels of type II collagen (COL II) and osteocalcin (OCN), sections of Alg and Alg/FDM with hMSCs were incubated at 4 °C with the corresponding primary antibodies (Abcam, UK). After washing the sections with PBS, antibody staining was performed using secondary antibodies (Abcam, UK) according to the manufacturer's protocol. Then, the sections were incubated with 4′, 6′-diamidino-2-phenylindole (DAPI) (Thermo Fisher Scientific, USA) for the nucleus. The fluorescently labeled cells were finally observed under a LSM 700 laser scanning confocal microscope (Zeiss, Germany).

### 2.7. Quantitative real time RT-PCR

Total RNA was extracted from hydrogels prepared at different time points (1, 7 and 28 days) using Trizol reagent (Invitrogen, USA) according to the manufacturer's instructions. The extracted RNA was dissolved in nuclease-free water, and the RNA concentration was quantified using a NanoDrop ND1000 Spectrophotometer (Thermo Fisher Scientific). Complementary DNA synthesis was performed using Maxime RT PreMix (iNtRon, Korea) following the manufacturer's instructions. All polymerase chain reaction was carried out using ABI Prism 7500 (Applied Biosystems) and gene expression level was quantified using SYBR Premix Ex Taq (TaKaRa, Japan). Relative gene expression level was calculated by the comparative Ct method. All target primer sequences were received from Bioneer (Korea). Alkaline phosphatase (ALP, P324388), runt-related transition factor 2 (Runx2, P229954), OCN (P128146), Sry-related high-mobility-group box 9 (SOX9, P232240), COLII (298511), type X collagen (COLX, P261909) and Glyceraldehyde 3-phosphate dehydrogenase (GAPDH, P267613) are commercially available.

Sulfated glycosaminoglycan (sGAG) and calcium content

To determine the sGAG content in hMSCs encapsulated Alg and Alg/FDM hydrogels, each sample was digested in papain solution. Then sGAG content was then measured using a 1, 9-dimethyl-methylene blue (DMB) (Sigma-Aldrich, USA) assay in 96 well plates. Chondroitin sulfate C was used as a standard. The quantification of calcium deposition in the Alg and Alg/FDM hydrogels was investigated using a QuantiChrom Calcium Assay Kit (BioAssay Systems, USA) according to the manufacturer's instructions.

### 2.8. Scanning electron microscopy

The SEM image of Alg and Alg/FDM hydrogels with hMSCs was obtained after the samples kept at −80 °C, and then freeze-dried. SEM images were then acquired using Phenom Pro desktop SEM (Phenom-World, Netherland) and FE-SEM Hitachi S 4100 (Hitachi, Japan).

### 2.9. Statistical analysis

Quantitative data were expressed as mean ± standard error of the mean (SE). The significance of differences in the mean values was evaluated using the one-way ANOVA with Tukey tests. An asterisk denotes statistical significance as follows: *$p < 0.05$, **$p < 0.01$, or ***$p < 0.001$. All results were presented as mean ± standard deviation ($n = 3$ or 5) and were representative of three independent experiments.

## 3. Results and discussion

### 3.1. Preparation of alg and Alg/FDM hydrogels

FDM is prepared following a standardized decellularization technique using the mixture of Triton X-100 and $NH_4OH$ as the detergent and DNase/RNase, which is schematically illustrated in Fig. 1A (Subbiah et al., 2016). FDM was collected from a culture dish using a scraper and mixed homogeneously with hMSCs and aqueous Alg solution prior to crosslinking. FDM is enriched with biochemical and biophysical cues that can be potentially used to replace a cell adhesion domain such as RGD. The scanning electron microscopy (SEM) image showed an interconnected micro/nanofibrous structure of FDM and the diameter of the FDM fibers is measured to be 0.1–2 μm (Fig. 1G). Alg is a polysaccharide biopolymer consisting of mannuronic acid and glucuronic acid, usually obtained from seaweed and bacterial sources that are a widely used biopolymer in tissue engineering due to its biocompatibility, biodegradability, and ability to fabricate as a 3D scaffold and administer in the body (Lee & Mooney, 2012). Alg is readily crosslinked with divalent cation such as $Ca^{2+}$ and the mechanical

properties can be improved by fillers without compromising its physicochemical properties (Sun & Tan, 2013). 1 wt.% HMW and LMW Alg at 1:1 ratio was used for the fabrication of hydrogel. LMW Alg was prepared using γ-irradiation of HMW Alg. The average MW of both HMW and LMW Alg was found to be $245 \times 10^3$ g/mol and $84 \times 10^3$ g/mol (Table 1), respectively. FDM mixed Alg solution has further coalesced with hMSCs and crosslinking agent $CaSO_4$ slurry vigorously using a double syringe method while enough attention is paid to avoid bubble formation in the hydrogel. The schematic and gross appearance of 3D Alg/FDM/hMSCs hydrogel (CiB) is shown in Fig. 1B and C, respectively. The cloudy spots in the near transparent Alg hydrogel indicate FDM and the bright spots denote $CaSO_4$ slurry (Fig. 1C). The presence of bioactive FDM in a 3D oriented manner inside the Alg gel is evinced by the immunofluorescence staining of major ECM protein FN and Col I as displayed in Fig. 1D. It is noteworthy that the ECM fibrous structure is secured in the Alg gel. The mechanical properties of Alg were measured as a means of crosslinking density varying from 12.5 mM to 100 mM $CaSO_4$ (Fig. 1E). A concentration-dependent storage modulus change of Alg gel was also observed. The storage modulus of Alg mixed with 12.5 mM and 100 mM $CaSO_4$ is found to be 10 Pa and 10 kPa, respectively, and indicates that the storage modulus is directly proportional to crosslinking density. The cross-linking of Alg by $CaSO_4$ slurry is saturated in less than an hour after mixing (Fig. 1E). This indicates that the undissolved $CaSO_4$ particles may not have direct effect on the bulk mechanical properties of Alg hydrogel. Meanwhile, hMSCs distribution and viability was investigated using calcein acetoxymethyl ester (AM) staining and the z-stack confocal imaging system. The result shows that more than 95% of encapsulated cells are viable, which proves that the used $CaSO_4$ concentration did not deteriorate the cell viability. Moreover, the encapsulated cells are uniformly distributed throughout the Alg hydrogel (Fig. 1F). These results indicate that Alg/FDM hydrogel provides a natural ECM mimicking microenvironment with biochemical and biophysical cues, and offers a highly interacting 3D platform for encapsulated hMSCs.

**Table 1**
Average MW and PDI of HMW and LMW Alg, measured using GPC.

| Sample | Avg. MW | PDI |
|---|---|---|
| HMW | $245 \times 10^3$ | 1.3 |
| LMW | $84 \times 10^3$ | 1.6 |

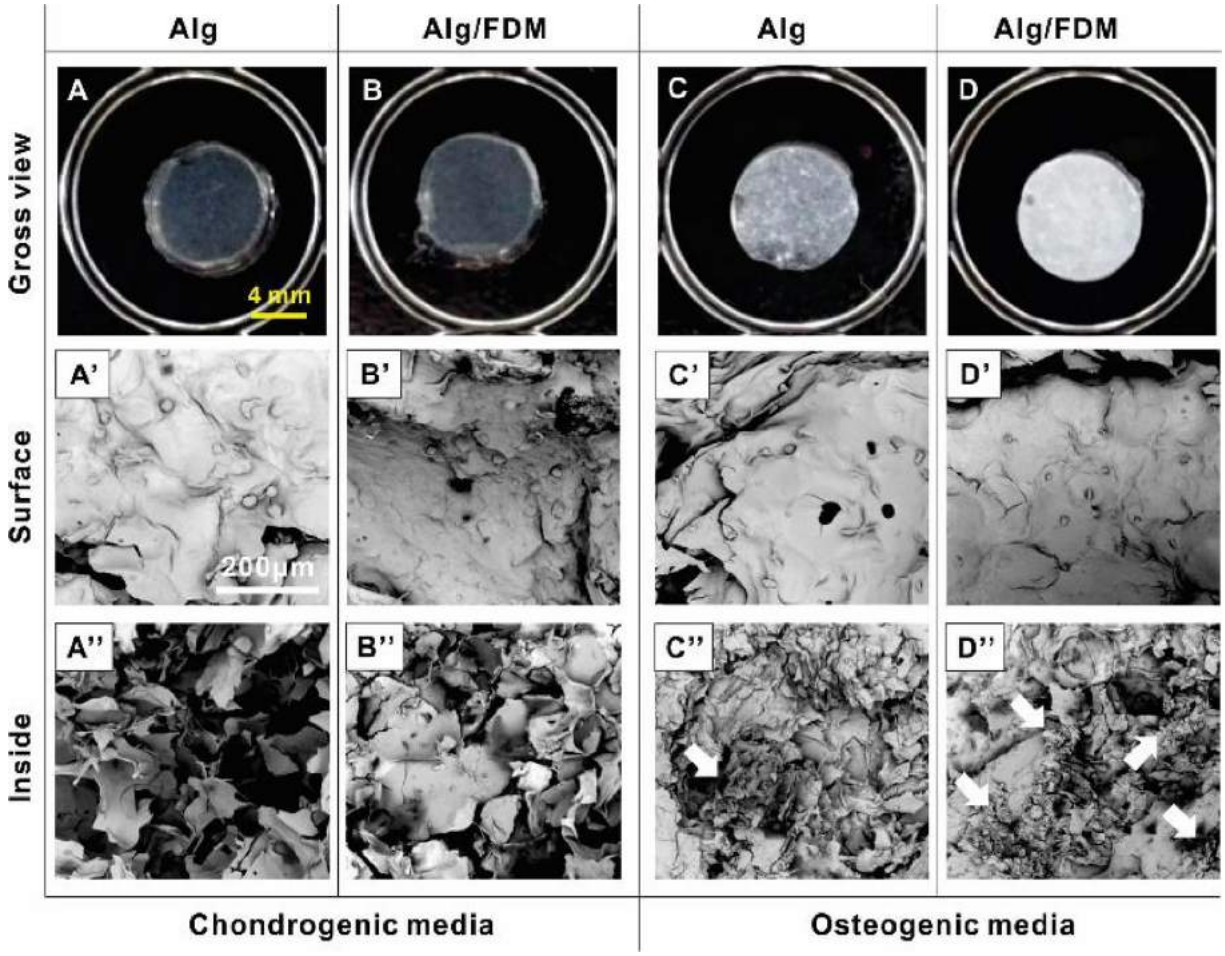


**Fig. 2.** Gross view, surface and cross section SEM images of Alg-hMSCs (A, A', A") Alg/FDM-hMSCs (B, B', B") in chondrogenic media, and Alg-hMSCs (C, C', C") Alg/FDM-hMSCs (D, D', D") in osteogenic media taken at 28th day, respectively. The gel formed *in situ* at 37 °C was quenched in −80 °C, followed by freeze-drying. The scale bar is 200 μm. Red arrows indicate small mineral deposits.

### 3.2. Chondrogenic and osteogenic differentiation of hMSCs

#### 3.2.1. Morphological characterization of alg and Alg/FDM hydrogels

The gross appearance of the Alg and Alg/FDM hydrogels are shown in Fig. 2A–D. The photographs were produced gels at 28 days in chondrogenic and osteogenic induction media, respectively. During the culture with osteogenic induction media, Alg and Alg/FDM hydrogels showed a transparent-to-white color transition as seen in Fig. 2C and D. However, Alg and Alg/FDM hydrogel in chondrogenic induction media maintained a transparent color. Fig. 2A'–D' and A"–D" show SEM images of respective gels that are cultured in chondrogenic and osteogenic media. The outer region of the hydrogel demonstrated a smooth surface and the presence of several cells irrespective of the culture media. However, the inner region of hydrogel cultured in chondrogenic induction media displayed large pores and sheet-like morphology, and the hydrogel cultured in osteogenic induction media displayed small particles with cells denoted by arrows. The results indicate that chondrogenic and osteogenic induction display different output in the hydrogel.

#### 3.2.2. Cell viability and proliferation

The hMSCs were cultured in the *in situ* formed gel by using specific differentiation media inducing chondrogenesis and osteogenesis. Live and dead cell assay was conducted to investigate cell viability during the 3D culture of the hMSCs by staining live cells (green) and dead cells (red). Over the 28 days of incubation, the hMSCs in the gels showed excellent viability in all incubating conditions of chondrogenic and osteogenic induction media (Fig. 3A and B). The cell proliferation increased about three and four times over 7 days of incubation in the chondrogenic and osteogenic induction media, respectively (Fig. 3C and D). However, cell proliferation decreased and maintained after 14 days in the chondrogenic induction media. Our results prove that Alg hydrogel and FDM offer more biomimetic conditions for survival and growth of hMSCs and have lower toxicity and immunogenic effect than popular synthetic matrices such as poly(acrylamide), poly(vinyl alcohol), and N-isopropylacrylamide (Bae et al., 2012; Subbiah et al., 2016). In other words, our platform offers a stable environment as a matrix for 3D cell culture for controlling stem cell survival.

#### 3.2.3. Biomarkers for differentiation

To determine chondrogenic and osteogenic differentiation, we observed immunofluorescence and histological staining. Type II collagen (COL II) and osteocalcin (OCN) immunofluorescence staining of hMSCs encapsulated in the 3D hydrogel matrix was carried out to further evaluate the potential of chondrogenesis and osteogenesis, respectively. COL II and OCN appeared as a green color and the 4′-6- diamidino-2-phenylindole (DAPI) stained nucleus as a blue color by immunofluorescence staining (Figs. 4A and 5 A). Positive staining of COL II and OCN was found to be higher in Alg/FDM hydrogels than bare Alg. Tissue-specific ECM production in the 3D hydrogel matrix by differentiated cells was analyzed by evaluating the histological staining such as sulfated glycosaminoglycan (sGAGs) contents and calcium. Compared with hMSCs cultured in the bare Alg hydrogel without FDM, a substantial expression of sGAGs was seen as a stained blue color in the

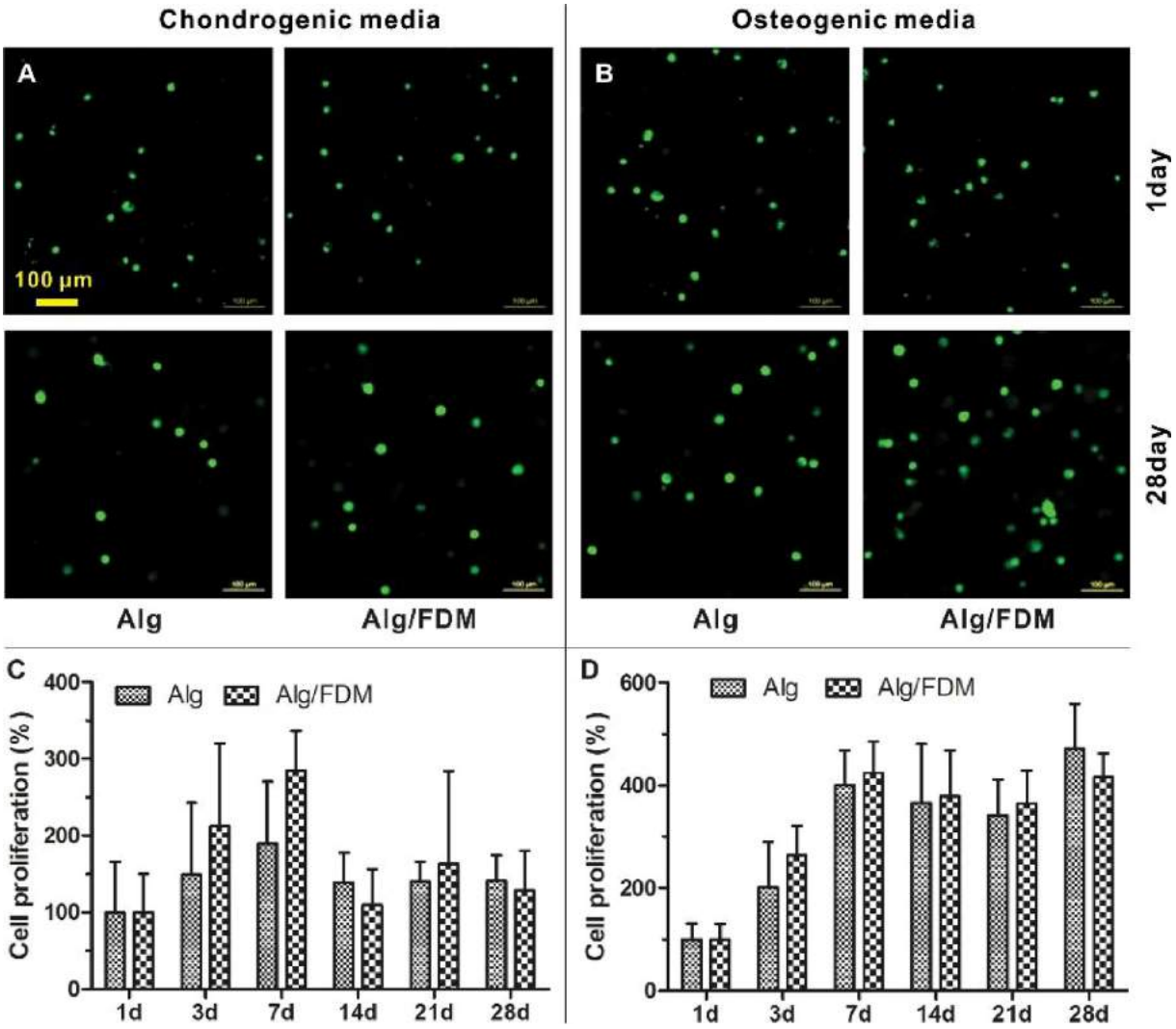


**Fig. 3.** (A, B) Viability and (C, D) proliferation of cells in Alg and Alg/FDM analyzed by the live/dead cell and CCK-8 assay. The results of each date were compared in the chondrogenic and osteogenic induction media, respectively. The scale bar is 100 μm.

presence of FDM in Alg/FDM hydrogels (Fig. 4B and D). On the other hand, alizarin red and von Kossa staining demonstrated comparatively strong staining for minerals and calcium deposits for Alg/FDM hydrogels than bare Alg hydrogel (Fig. 5B, C, and E). Likewise, the amount of sGAGs and calcium deposits were found to be significantly higher in the presence of FDM of the Alg/FDM hydrogels (Figs. 4D and 5 E). These results show that the CiB platform induces the tissue-specific differentiation including chondrogenesis and osteogenesis by adding FDM in Alg hydrogel.

#### 3.2.4. Gene expression

We examined quantitative real time RT-PCR to further confirm the chondrogenic and osteogenic differentiation potential of encapsulated hMSCs in Alg and Alg/FDM hydrogels. The mRNA expression of SOX9 (early), COL II (middle/late), and COL X (late/hypertrophy) in Alg and Alg/FDM hydrogels with chondrogenic induction media were observed (Fig. 4C). The Alg/FDM group showed higher expression of SOX9 and COL II. However, a small expression level of COL X that is mainly expressed in hypertrophic chondrocytes, was observed for Alg/FDM hydrogel than the bare Alg group. Specific genes of osteogenic differentiation including ALP (early/middle), RUNX-2 (early) and OCN (late) were investigated for the hMSCs cultured with the osteogenic induction media (Fig. 5D). The ALP and RUNX-2 expression level in Alg/FDM hydrogels was higher than the bare Alg hydrogels at the early stage and OCN expression level at 28 days was found to be similar between Alg and Alg/FDM hydrogels. Thus, we determined the chondrogenesis and osteogenesis potential of hMSCs in Alg hydrogel and the role of FDM in Alg hydrogel on the improvement of cell adhesion, viability, proliferation and controlling stem cell differentiation by providing a natural ECM biomimicking 3D microenvironment platform.

### 3.3. Mineralization for osteogenic differentiation

Field-emission (FE) SEM and energy-dispersive X-ray spectroscopy (EDS) analyses were performed to determine the osteogenic differentiation by observing the bone nodules-like structure in the hydrogel. FE-SEM images show plenty of mineralized bone nodules in Alg/FDM than bare Alg hydrogel (Fig. 6A). The production of minerals is principally bioapatites in the form of globular accretions as reported in previous studies (Abagnale et al., 2015). They showed the different size, dispersion and calcium amounts of Alg and Alg/FDM hydrogel by FE-SEM and EDS analyses. Consequently, we observed that Alg/FDM hydrogel show more opaque color than bare Alg hydrogel. In addition, the ECM fiber formation on cells and bone nodules in the Alg/FDM hydrogel was witnessed by a magnified image (Fig. 6C). The results suggest that our system significantly induce osteogenic differentiation of hMSCs by forming ECM fiber and bone nodules in Alg/FDM hydrogel.

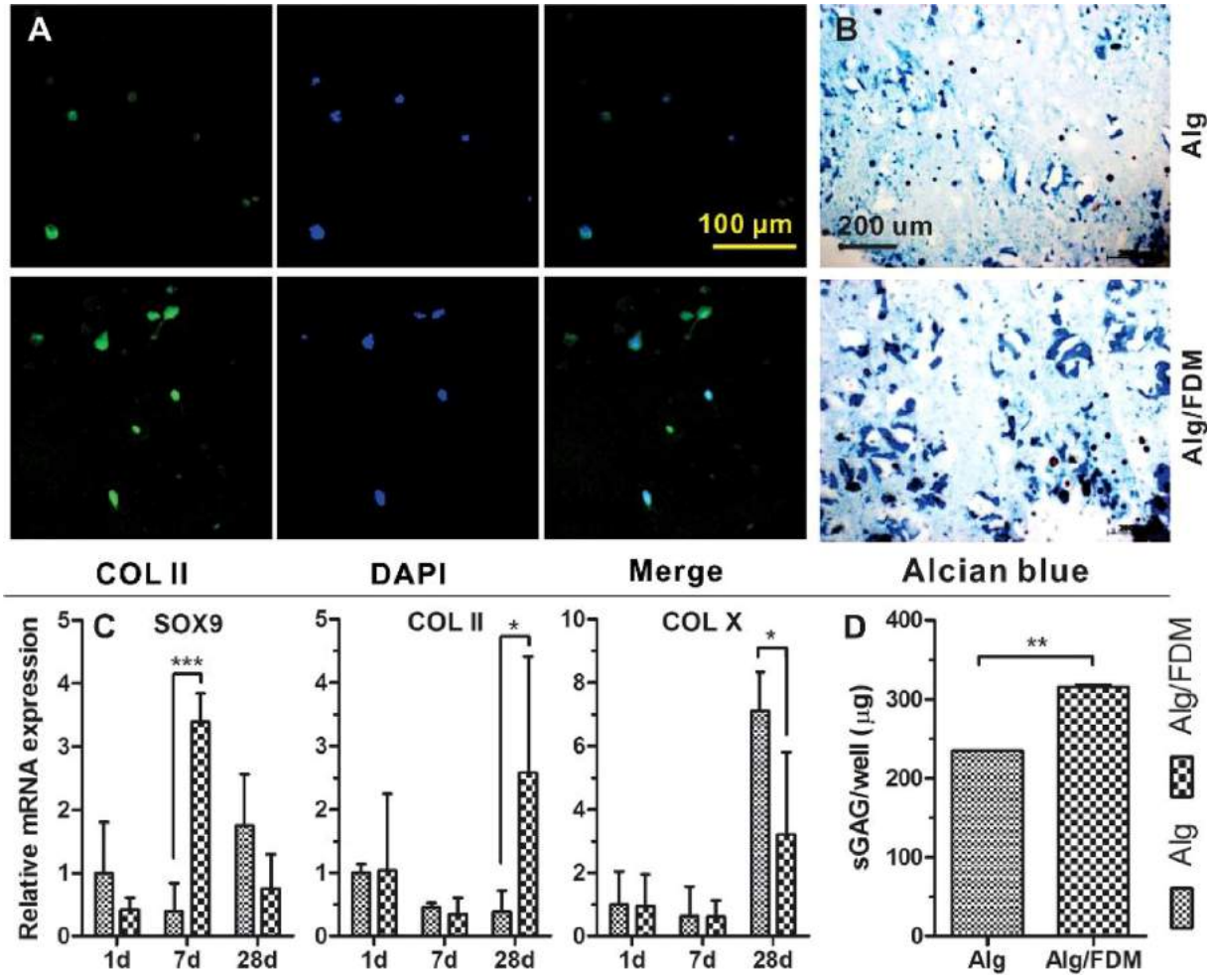


**Fig. 4.** (A) Immunofluorescence stained images for chondrogenesis (COL II) are shown. Nucleus was stained by DAPI. The scale bar is 100 μm. All samples were maintained for 28th day in the chondrogenic induction media. (B) Histological staining of Alg and Alg/FDM by alcian blue staining method. (C) Gene expression of hMSCs in 3D-cultured samples analysed by real time RT-PCR. The biomarkers for chondrogenesis (Sox9, COL II, and COLX) are shown. The data were normalized by the GAPDH and 1 day data. The data are presented as the mean ± SD of three independent experiments. (D) The amount of sGAG as a function of FDM measured using the DMB assay. The data are presented as the mean ± SD of three independent experiments. * and ** indicate $P < 0.01$ and $P < 0.05$, respectively.

### 3.4. Cues-integrated-biomaterials (CiB)

Biomaterials, as described by the European Society, are materials intended to interface with biological systems to evaluate, treat, augment, or replace organs, tissues, or functions of the body (O'Brien, 2011). Collagen, gelatin, fibrinogen, keratin, silk, Alg, chitosan, glycosaminoglycans, and cellulose are the most prevalent naturally derived biomaterials (Akter, 2016; Prasad Shastri & Lendlein, 2011; Uebersax, Merkle, & Meinel, 2009). Alg, in particular, has gained popularity in regenerative medicine due to its biocompatibility, biodegradability, durability, injectability, and biomolecule diffusivity, as well as its application in the fabrication and functionalization of 3D scaffolds with desired chemical groups. Alg has been tested for GF/cell delivery in scaffolds and stiffness-tunable cell culture platforms (Subbiah et al., 2015; Sun & Tan, 2013; Venkatesan, Bhatnagar, Manivasagan, Kang, & Kim, 2015). However, Alg lacks cell-adhesive moieties and ECM-mimicking topography limits its stem cell-based therapeutic applications. Functionalization of biomaterials using ECM biomolecules such as FN and cell adhesive moieties such as RGD peptide are reported to enhance cell adhesion and survival (Degala et al., 2011; Evangelista et al., 2007; Park & Lee, 2011). However, there is a limit to provide biophysical cues. Recent reports note the roles of biophysical and biochemical cues such as elasticity, topography, GFs, and ECM proteins in the survival, proliferation, and differentiation of stem cells into tissue-specific lineages (Engler, Sen, Sweeney, & Discher, 2006; Guilak et al., 2009; Higuchi, Ling, Chang, Hsu, & Umezawa, 2013; Pittenger et al., 1999; Pompe, Salchert, Alberti, Zandstra, & Werner, 2010; Subbiah et al., 2015, 2016). FDM accurately mimics the complexity of natural ECM, and provides biophysical and biochemical cues. Our group has previously demonstrated FDM as a carrier for GFs delivery (Du, Hwang et al., 2014) and the role of stiffness tunable FDM on the multi-lineage differentiation of hMSCs, vascular morphogenesis of human endothelial cells, and cardiomyogenesis of cardiomyoblasts (Subbiah et al., 2016). Hence, we developed 3D FDM-integrated Alg hydrogels (CiB), which fully conserve cell adhesive topography, ECM biomolecules, and spatial orientation for cells growth and proliferation. Results in this study indicate that CiBs have a greater positive effect than bare Alg hydrogel matrix on survival and proliferation, as well as osteogenic and chondrogenic differentiation of hMSCs. Therefore, CiBs are a promising alternative to both bare and functionalized Alg in tissue engineering and regenerative medicine applications.

## 4. Conclusions

hMSCs were encapsulated in the *in situ* formed Alg and Alg/FDM hydrogel. The chondrogenic and osteogenic differentiation potential of encapsulated hMSCs in the Alg hydrogel was investigated in the absence or presence of FDM along with the presence of differential growth

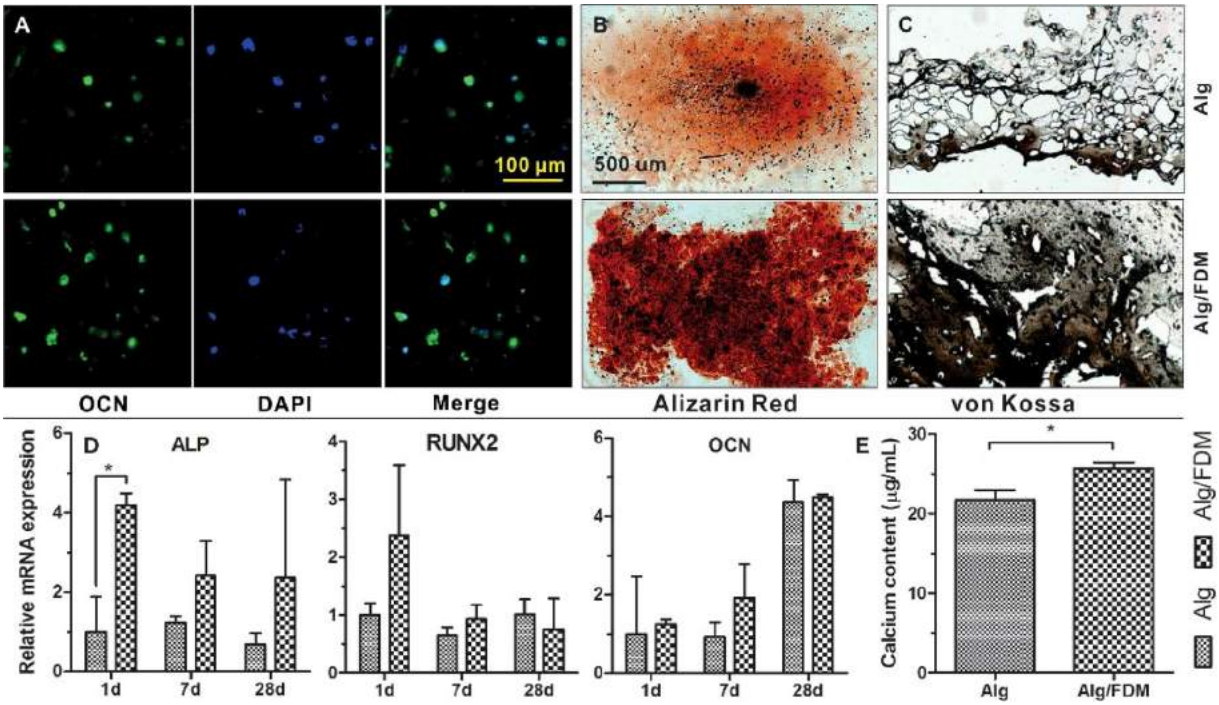


**Fig. 5.** (A) Immunofluorescence stained images for osteogenesis (OCN) are shown. Nucleus was stained by DAPI. The scale bar is 100 μm. All samples were maintained for 28th day in the osteogenic induction media. Histological staining of Alg and Alg/FDM by (B) alizarin red S and (C) von kossa staining method. (D) Gene expression of hMSCs in 3D-cultured samples analysed by real time RT-PCR. The biomarkers for osteogenesis (ALP, Runx2, and OCN) are shown. The data were normalized by the GAPDH and 1 day data. The data are presented as the mean ± SD of three independent experiments. (E) The amount of calcium as a function of FDM measured using the Quantichrom Calcium assay. The data are presented as the mean ± SD of three independent experiments. * and ** indicate $P < 0.01$ and $P < 0.05$, respectively.

factors. The cells in the Alg and Alg/FDM hydrogel showed a different cell proliferation pattern and produced tissue-specific markers. Particularly, hMSCs encapsulated in Alg/FDM hydrogel showed a significantly higher expression of chondrogenic and osteogenic biomarkers *in vitro*. Thus, Alg/FDM hydrogel proved to be a suitable candidate for transplanting hMSCs to induce chondrogenic and osteogenic differentiation and to act as a novel CiB. In conclusion, this study presents a 3D culture system of an Alg/FDM hydrogel matrix and suggests that FDM in an Alg hydrogel can control differentiation of stem cells into a specific lineage and envision its potential tissue regeneration applications.

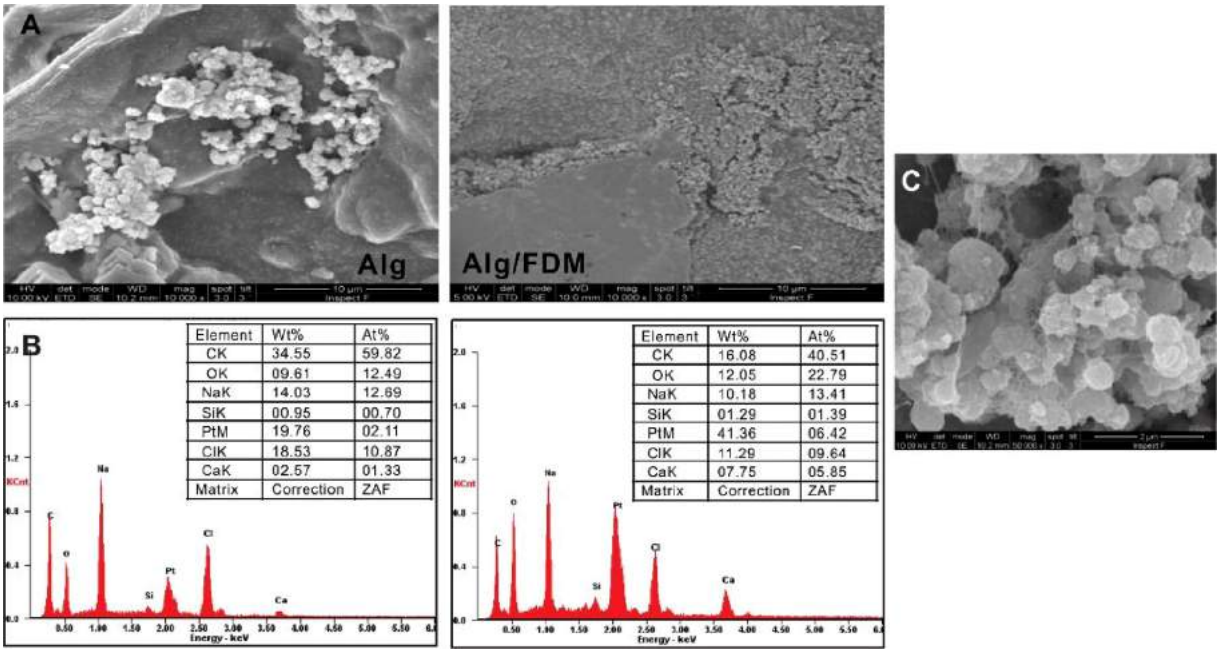


**Fig. 6.** (A) FE-SEM images and (B) EDS analysis of Alg and Alg/FDM formed *in situ* at 37 °C was quenched −80 °C, followed by freeze-drying. The scale bar is 10 μm. (C) The high magnification image of mineralized bone nodules and ECM fibers on the cell surfaces within Alg/FDM. The scale bar is 2 μm.

## Acknowledgements

This work was supported by the National Research Foundation of Korea (NRF) grant funded by Korea government (MSIT) (2018R1C1B6002333, 2016M3A9B4919711). This work was also supported by Korea Health Industry Development Institute (KHIDI), funded by the Ministry of Health and Welfare, Republic of Korea (HI16C0133).

## References

Akter, F. (2016). *Chapter 2 - Principles of tissue engineering. Tissue engineering made easy*. Academic Press3–16.

Bae, S. E., Bhang, S. H., Kim, B. S., & Park, K. (2012). Self-assembled extracellular macromolecular matrices and their different osteogenic potential with preosteoblasts and rat bone marrow mesenchymal stromal cells. *Biomacromolecules, 13*(9), 2811–2820.

Blanpain, C., Lowry, W. E., Geoghegan, A., Polak, L., & Fuchs, E. (2004). Self-renewal, Multipotency, and the existence of two cell populations within an epithelial stem cell niche. *Cell, 118*(5), 635–648.

Busilacchi, A., Gigante, A., Mattioli-Belmonte, M., Manzotti, S., & Muzzarelli, R. A. A. (2013). Chitosan stabilizes platelet growth factors and modulates stem cell differentiation toward tissue regeneration. *Carbohydrate Polymers, 98*(1), 665–676.

Choi, D. H., Suhaeri, M., Hwang, M. P., Kim, I. H., Han, D. K., & Park, K. (2014). Multilineage differentiation of human mesenchymal stromal cells on the biophysical microenvironment of cell-derived matrix. *Cell and Tissue Research, 357*(3), 781–792.

Crapo, P. M., Gilbert, T. W., & Badylak, S. F. (2011). An overview of tissue and whole organ decellularization processes. *Biomaterials, 32*(12), 3233–3243.

Degala, S., Zipfel, W. R., & Bonassar, L. J. (2011). Chondrocyte calcium signaling in response to fluid flow is regulated by matrix adhesion in 3-D alginate scaffolds. *Archives of Biochemistry and Biophysics, 505*(1), 112–117.

Delcroix, G. J. R., Schiller, P. C., Benoit, J.-P., & Montero-Menei, C. N. (2010). Adult cell therapy for brain neuronal damages and the role of tissue engineering. *Biomaterials, 31*(8), 2105–2120.

Du, P., Hwang, M. P., Noh, Y. K., Subbiah, R., Kim, I. G., Bae, S. E., ... Park, K. (2014). Fibroblast-derived matrix (FDM) as a novel vascular endothelial growth factor delivery platform. *Journal of Controlled Release: Official Journal of the Controlled Release Society, 194c*, 122–129.

Du, P., Subbiah, R., Park, J. H., & Park, K. (2014). Vascular morphogenesis of human umbilical vein endothelial cells on cell-derived macromolecular matrix microenvironment. *Tissue Engineering Part A, 20*(17-18), 2365–2377.

Elbert, D. L. (2011). Bottom-up tissue engineering. *Current Opinion in Biotechnology, 22*(5), 674–680.

Engler, A. J., Sen, S., Sweeney, H. L., & Discher, D. E. (2006). Matrix elasticity directs stem cell lineage specification. *Cell, 126*(4), 677–689.

Evangelista, M. B., Hsiong, S. X., Fernandes, R., Sampaio, P., Kong, H.-J., Barrias, C. C., ... Granja, P. L. (2007). Upregulation of bone cell differentiation through immobilization within a synthetic extracellular matrix. *Biomaterials, 28*(25), 3644–3655.

Fischer, R. S., Myers, K. A., Gardel, M. L., & Waterman, C. M. (2012). Stiffness-controlled three-dimensional extracellular matrices for high-resolution imaging of cell behavior. *Nature Protocols, 7*(11), 2056–2066.

Fitzpatrick, L. E., & McDevitt, T. C. (2015). Cell-derived matrices for tissue engineering and regenerative medicine applications. *Biomaterials Science, 3*(1), 12–24.

Gattazzo, F., Urciuolo, A., & Bonaldo, P. (2014). Extracellular matrix: A dynamic microenvironment for stem cell niche. *Biochimica et Biophysica Acta, 1840*(8), 2506–2519.

Guilak, F., Cohen, D. M., Estes, B. T., Gimble, J. M., Liedtke, W., & Chen, C. S. (2009). Control of stem cell fate by physical interactions with the extracellular matrix. *Cell Stem Cell, 5*(1), 17–26.

Higuchi, A., Ling, Q.-D., Chang, Y., Hsu, S.-T., & Umezawa, A. (2013). Physical cues of biomaterials guide stem cell differentiation fate. *Chemical Reviews, 113*(5), 3297–3328.

Kong, H.-J., Lee, K. Y., & Mooney, D. J. (2002). Decoupling the dependence of rheological/mechanical properties of hydrogels from solids concentration. *Polymer, 43*(23), 6239–6246.

Kong, H. J., Smith, M. K., & Mooney, D. J. (2003). Designing alginate hydrogels to maintain viability of immobilized cells. *Biomaterials, 24*(22), 4023–4029.

Kshitiz, P. J., Kim, P., Helen, W., Engler, A. J., Levchenko, A., & Kim, D.-H. (2012). Control of stem cell fate and function by engineering physical microenvironments. *Integrative Biology, 4*(9), 1008.

Lee, K. Y., & Mooney, D. J. (2012). Alginate: Properties and biomedical applications. *Progress in Polymer Science, 37*(1), 106–126.

Lee, K., Silva, E. A., & Mooney, D. J. (2011). Growth factor delivery-based tissue engineering: General approaches and a review of recent developments. *Journal of the Royal Society Interface, 8*(55), 153–170.

Lehr, E. J., Rayat, G. R., Chiu, B., Churchill, T., McGann, L. E., Coe, J. Y., ... Ross, D. B. (2011). Decellularization reduces immunogenicity of sheep pulmonary artery vascular patches. *The Journal of Thoracic and Cardiovascular Surgery, 141*(4), 1056–1062.

McNamara, L. E., McMurray, R. J., Biggs, M. J. P., Kantawong, F., Oreffo, R. O. C., & Dalby, M. J. (2010). Nanotopographical control of stem cell differentiation. *Journal of Tissue Engineering, 2010*, 120623.

Morais, D. S., Rodrigues, M. A., Silva, T. I., Lopes, M. A., Santos, M., Santos, J. D., ... Botelho, C. M. (2013). Development and characterization of novel alginate-based hydrogels as vehicles for bone substitutes. *Carbohydrate Polymers, 95*(1), 134–142.

O'Brien, F. J. (2011). Biomaterials & scaffolds for tissue engineering. *Materials Today, 14*(3), 88–95.

Ottone, C., Krusche, B., Whitby, A., Clements, M., Quadrato, G., Pitulescu, M. E., ... Parrinello, S. (2014). Direct cell–cell contact with the vascular niche maintains quiescent neural stem cells. *Nature Cell Biology, 16*(11), 1045–1056.

Park, H., & Lee, K. Y. (2011). Facile control of RGD-alginate/hyaluronate hydrogel formation for cartilage regeneration. *Carbohydrate Polymers, 86*(3), 1107–1112.

Park, M. H., Yu, Y., Moon, H. J., Ko, D. Y., Kim, H. S., Lee, H., ... Jeong, B. (2014). 3D culture of tonsil-derived mesenchymal stem cells in poly(ethylene glycol)-Poly(l-alanine-co-l-phenyl alanine) thermogel. *Advanced Healthcare Materials, 3*(11), 1782–1791.

Pilipchuk, S. P., Vaicik, M. K., Larson, J. C., Gazyakan, E., Cheng, M.-H., & Brey, E. M. (2013). Influence of crosslinking on the stiffness and degradation of dermis-derived hydrogels. *Journal of Biomedical Materials Research Part A, 101*(10), 2883–2895.

Pittenger, M. F., Mackay, A. M., Beck, S. C., Jaiswal, R. K., Douglas, R., Mosca, J. D., ... Marshak, D. R. (1999). Multilineage potential of adult human mesenchymal stem cells. *Science, 284*(5411), 143–147.

Pittenger, M. F., Mbalaviele, G., Black, M., Mosca, J. D., & Marshak, D. R. (2001). *Mesenchymal stem cells*. Kluwer academic publishers.

Place, E. S., Evans, N. D., & Stevens, M. M. (2009). Complexity in biomaterials for tissue engineering. *Nature Materials, 8*(6), 457–470.

Pompe, T., Salchert, K., Alberti, K., Zandstra, P., & Werner, C. (2010). Immobilization of growth factors on solid supports for the modulation of stem cell fate. *Nature Protocols, 5*(6), 1042–1050.

Prasad Shastri, V., & Lendlein, A. (2011). Engineering materials for regenerative medicine. *MRS Bulletin, 35*(8), 571–577.

Rehmann, M. S., Luna, J. I., Maverakis, E., & Kloxin, A. M. (2016). Tuning microenvironment modulus and biochemical composition promotes human mesenchymal stem cell tenogenic differentiation. *Journal of Biomedical Materials Research Part A, 104*(5), 1162–1174.

Reilly, G. C., & Engler, A. J. (2010). Intrinsic extracellular matrix properties regulate stem cell differentiation. *Journal of Biomechanics, 43*(1), 55–62.

Rowley, J. A., Madlambayan, G., & Mooney, D. J. (1999). Alginate hydrogels as synthetic extracellular matrix materials. *Biomaterials, 20*(1), 45–53.

Simó, G., Fernández-Fernández, E., Vila-Crespo, J., Ruipérez, V., & Rodríguez-Nogales, J. M. (2017). Research progress in coating techniques of alginate gel polymer for cell encapsulation. *Carbohydrate Polymers, 170*(Supplement C), 1–14.

Simons, B. D., & Clevers, H. (2011). Strategies for homeostatic stem cell self-renewal in adult tissues. *Cell, 145*(6), 851–862.

Slaughter, B. V., Khurshid, S. S., Fisher, O. Z., Khademhosseini, A., & Peppas, N. A. (2009). Hydrogels in regenerative medicine. *Advance Materials, 21*(32-33), 3307–3329.

Subbiah, R., Du, P., Hwang, M., Kim, I., Van, S., Noh, Y., ... Park, K. (2014). Dual growth factor-loaded core-shell polymer microcapsules can promote osteogenesis and angiogenesis. *Macromolecular Research,* 1–10.

Subbiah, R., Hwang, M. P., Du, P., Suhaeri, M., Hwang, J. H., Hong, J. H., ... Park, K. (2016). Tunable crosslinked cell-derived extracellular matrix guides cell fate. *Macromolecular Bioscience, 16*(11), 1723–1734.

Subbiah, R., Hwang, M. P., Van, S. Y., Do, S. H., Park, H., Lee, K., ... Park, K. (2015). Osteogenic/angiogenic dual growth factor delivery microcapsules for regeneration of vascularized bone tissue. *Advanced Healthcare Materials, 4*(13), 1982–1992.

Sun, J., & Tan, H. (2013). Alginate-based biomaterials for regenerative medicine applications. *Materials (Basel, Switzerland), 6*(4), 1285–1309.

Tibbitt, M. W., & Anseth, K. S. (2009). Hydrogels as extracellular matrix mimics for 3D cell culture. *Biotechnology and Bioengineering, 103*(4), 655–663.

Trappmann, B., Gautrot, J., Connelly, J., Strange, D., Li, Y., Oyen, M., ... Huck, W. (2012). Extracellular-matrix tethering regulates stem-cell fate. *Nature Materials, 11*(7), 642–649.

Uebersax, L., Merkle, H. P., & Meinel, L. (2009). Biopolymer-based growth factor delivery for tissue repair: From natural concepts to engineered systems. *Tissue Engineering Part B: Reviews, 15*(3), 263–289.

Venkatesan, J., Bhatnagar, I., Manivasagan, P., Kang, K.-H., & Kim, S.-K. (2015). Alginate composites for bone tissue engineering: A review. *International Journal of Biological Macromolecules, 72*, 269–281.

Wen, J. H., Vincent, L. G., Fuhrmann, A., Choi, Y. S., Hribar, K. C., Taylor-Weiner, H., ... Engler, A. J. (2014). Interplay of matrix stiffness and protein tethering in stem cell differentiation. *Nature Materials, 13*(10), 979–987.

White, L. J., Saldin, L. T., Keane, T. J., Cramer, M. C., Shakesheff, K. M., & Badylak, S. F. (2017). *2.24 hydrogels of decellularized matrix A2 - Ducheyne, Paul. Comprehensive biomaterials II*. Oxford: Elsevier532–541.

Willett, N. J., Thote, T., Lin, A. S. P., Moran, S., Raji, Y., Sridaran, S., ... Guldberg, R. E. (2014). Intra-articular injection of micronized dehydrated human amnion/chorion membrane attenuates osteoarthritis development. *Arthritis Research & Therapy, 16*(1), R47.

Wylie, R. G., Ahsan, S., Aizawa, Y., Maxwell, K. L., Morshead, C. M., & Shoichet, M. S. (2011). Spatially controlled simultaneous patterning of multiple growth factors in three-dimensional hydrogels. *Nature Materials, 10*(10), 799–806.

Yang, J.-S., Xie, Y.-J., & He, W. (2011). Research progress on chemical modification of alginate: A review. *Carbohydrate Polymers, 84*(1), 33–39.